Anomalous Lattice Dynamics of $EuSi_2$ Nanoislands: Role of Interfaces Unveiled

A. Seiler,[1,2] P. Piekarz,[3] S. Ibrahimkutty,[1,2,†] D. G. Merkel,[4,‡] O. Waller,[1,2,§] R. Pradip,[1,2] A. I. Chumakov,[4] R. Rüffer,[4] T. Baumbach,[1,2,5] K. Parlinski,[3] M. Fiederle,[6] and S. Stankov[2,1,*]

[1]*Laboratory for Applications of Synchrotron Radiation, Karlsruhe Institute of Technology, D-76131 Karlsruhe, Germany*
[2]*Institute for Photon Science and Synchrotron Radiation, Karlsruhe Institute of Technology, D-76344 Eggenstein-Leopoldshafen, Germany*
[3]*Institute of Nuclear Physics, Polish Academy of Sciences, PL-31342 Kraków, Poland*
[4]*ESRF-The European Synchrotron, F-38000 Grenoble, France*
[5]*ANKA Synchrotron Radiation Facility, Karlsruhe Institute of Technology, D-76344 Eggenstein-Leopoldshafen, Germany*
[6]*Freiburg Materials Research Center, University of Freiburg, D-79104 Freiburg, Germany*

(Received 27 July 2016; published 28 December 2016)

We report a systematic lattice dynamics study of $EuSi_2$ films and nanoislands by *in situ* nuclear inelastic scattering on ^{151}Eu and *ab initio* theory. The Eu-partial phonon density of states of the nanoislands exhibits anomalous excess of phonon states at low and high energies, not present in the bulk and at the $EuSi_2(001)$ surface. We demonstrate that atomic vibrations *along* the island-substrate interface give rise to phonon states both at low and high energies, while atomic vibrations *across* the island-island interface result in localized high-energy phonon modes.

DOI: 10.1103/PhysRevLett.117.276101

Thermal lattice excitations in materials with dimensions at the nanometer length scale are drastically modified with respect to their bulk counterparts [1]. This gives rise to alterations of the phonon dispersions and density of states (DOS), and leads to anomalies in the thermodynamic and elastic properties of nanoscale materials [2]. Distinct features of their phonon DOS are enhancement of states at low and high energies and broadening, suppression, and shift of the peaks. In various nanosystems these anomalies have entirely different origin and strength. For instance, in bulk nanocrystalline materials they originate from the large fraction of disordered grain boundaries, while the vibrational properties of the nanograins remain bulklike [3–7]. Epitaxial strain and broken translational symmetry are the main sources of vibrational anomalies in thin films and surfaces [8–11]. DOS of nanoparticles revealed drastic size and shape effects that remain to a large extent unexplained [12–18]. 2D vibrational dynamics has theoretically been predicted [4,12] and experimentally observed in the DOS of nanocrystalline Pd [19], Fe nanoislands [16,18], and FeO films [20]. Despite the intense research, the impact of the abrupt change of atomic surroundings at the interface on the lattice dynamics has scarcely been investigated [9,21–23]. Elucidating this impact, however, is of high importance for the on-going efforts to control thermal properties of materials by nanoscaling [24]. Two fundamentally different approaches have been proposed [25]: (i) enhancing the diffuse (incoherent) phonon scattering by introducing impurities and interfaces; (ii) enhancing the interface specular (coherent) phonon reflection and transmission by using superlattices. The progress in either of these strategies requires a comprehensive understanding of the lattice dynamics of nanoscale interfaces.

At very low coverages metallic rare-earth disilicides self-organize on the Si surface in clusters, islands, and high aspect ratio nanowires [26]. They have been actively investigated due to the immense potential for applications in light emitting technology [27] and nanoelectronics as Ohmic contacts and interconnects in the integrated circuits [28]. The exceptionally low Schottky barrier height combined with the antiferromagnetic properties recently promoted europium disilicide ($EuSi_2$) to a prospective material for MOSFET technology [29]. However, the lattice dynamics of this material, which is of relevance to the proposed applications, remained unknown.

Here we present a systematic lattice dynamics study of epitaxial $EuSi_2$ bulklike film, thin film, and nanoislands by *in situ* nuclear inelastic scattering on ^{151}Eu and *ab initio* theory. The phonon DOS of the nanoislands exhibits anomalous enhancement at low and high energies, suppression, and broadening of the peaks. Our analysis demonstrates that the in-plane atomic vibrations *along* the island-substrate interface give rise to states at low and high energy, while the atomic vibrations *across* the island-island interface are essentially high-energy modes.

Epitaxial $EuSi_2$ samples with nominal Eu coverages of 20.0 (bulklike film), 5.0 (thin film), 1.0 (islands), and 0.26 (islands) nm, hereinafter referred to as *A*, *B*, *C*, and *D*, respectively, were prepared by deposition of metallic Eu on the vicinal Si(001) surface at 873 K and postgrowth annealing at 973 K for 10 min [30,33,34]. For the lowest coverages these growth conditions ensure the formation of islands with high surface density. An additional sample labeled *E*, with a coverage of 0.26 nm, was prepared by Eu deposition at 673 K and postgrowth annealing at 873 K for

10 min, resulting in the formation of isolated $EuSi_2$ islands with low surface density [33]. The *in situ* nuclear inelastic scattering experiment [35,36] was performed using the ultrahigh vacuum system [37] at the Nuclear Resonance beam line ID18 [38] of the ESRF on the nuclear transition in ^{151}Eu with energy 21.541 keV and an energy resolution of 1.2(1) meV [39]. The wave vector of the incident photon beam was kept parallel to the $EuSi_2[100]$, illuminating the samples at glancing angle of 0.12°. To suppress the multiphonon excitations all samples were measured at 100 K.

Figure 1 shows the Eu-partial DOS of samples *A*–*D* (left column) and the corresponding atomic-force microscopy (AFM) images (right column) of identical samples obtained in the home lab. The DOS of sample *A* is characterized by a localized peak at 12.5 meV, a low-energy tail and a sharp cutoff at 14.5 meV. This vibrational behavior is characteristic for a rattling mode of an atom locked in a cage [40]. Indeed, $EuSi_2$ exhibits a tetragonal $I4_1/amd$ structure with 4 Eu and 8 Si atoms in the unit cell [41]. Each Eu atom is surrounded by 12 Si atoms forming a cagelike configuration that confines the Eu atoms and leads to the observed Eu-partial DOS [30].

In addition to the peak at 12.5 meV, the DOS of sample *B* exhibits an enhancement of states at low energies, in particular a peak at 9 meV is clearly visible. The corresponding AFM image shows the formation of a film with rough surface suggesting an augmented contribution of vibrational states originating from the broken translational symmetry at the $EuSi_2(001)$ surface [11].

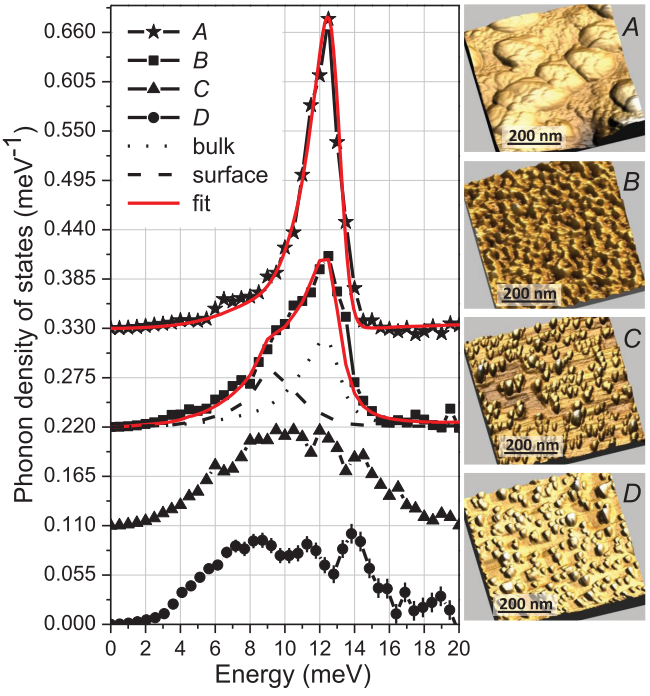

FIG. 1. The $EuSi_2[100]$ projected Eu-partial DOS of the investigated samples obtained at 100 K. The spectra are upshifted by 0.11 meV^{-1} for clarity. The dashed and dotted lines, respectively, depict the *ab initio* calculated surface and bulk Eu-partial DOS convoluted with the damped harmonic oscillator function, while the solid (red) lines stand for the fit (see text). The corresponding AFM images obtained in the home lab from identical samples are shown in the right column.

Furthermore, Fig. 1 reveals remarkable modifications of the Eu-partial DOS as the surface morphology evolves towards self-organized nanoislands. The DOS of sample *C* exhibits enhancement of states both at low and high energies, however, without a well-defined peak structure. Nevertheless, one can identify the bulk peak at 12 meV, as well as a broad peak at around 9 meV, and a peak onset at 14 meV. These features are even more pronounced in the DOS of sample *D* where the bulk peak is further suppressed and shifted to 11.5 meV, the augmented low-energy phonon states form a broad peak at around 8 meV and the peak at 14 meV is well defined. A high-energy tail extending up to 20 meV is also visible.

Density functional theory implemented in the VASP program [42] was employed to achieve a comprehensive understanding of the experimental observations. A $2\times2\times1$ supercell with 48 atoms was used to calculate the electronic and dynamic properties of bulk crystal, while an Eu-terminated $EuSi_2(001)$ surface was modeled by the thin slab approach [30]. Phonon dispersions along high-symmetry directions of the Brillouin zone and phonon DOS calculated with the direct method [43] for the bulk and Eu-terminated $EuSi_2(001)$ slab are plotted in Figs. 2(a) and 2(b), respectively. In agreement with the experimental observations for sample *A* (Fig. 1), the calculations confirm that the Eu-partial DOS contributes to the low-energy tail of the total DOS and the peak at 12.5 meV. Peaks at 21.6 and 24.2 meV arising from a coupling of the Eu vibrations to the optical modes of the neighboring Si atoms are also visible, being, however, about 20 times smaller in intensity compared to the main Eu peak. The total DOS of $EuSi_2$ extends up to 60 meV with the Si atoms contributing to the states with energies above 14 meV. Comparison of the calculated Eu-partial DOS (convoluted with a Gaussian function, FWHM = 1.2 meV) and the DOS of sample *A*, reveals a remarkable agreement between experiment and theory (Fig. 1).

The calculations disclose the presence of additional phonon dispersions in the slab that are not visible in bulk $EuSi_2$. They are particularly pronounced at low energies giving rise to the peak at 9.0 meV that originates from in-plane vibrational modes of the surface Eu atoms [Fig. 2(b)]. The atomic vibrations of the subsurface Eu layer remain very close to that of the bulk. Despite that the slab exhibits an Eu-terminated surface, pronounced changes are clearly visible in the vibrational dynamics of the subsurface Si atoms. This is a direct consequence of the broken translational symmetry at the surface that alters the interlayer distances in the entire slab.

Complete understanding of the DOS of sample *B* is achieved by combining the calculated DOS of the surface

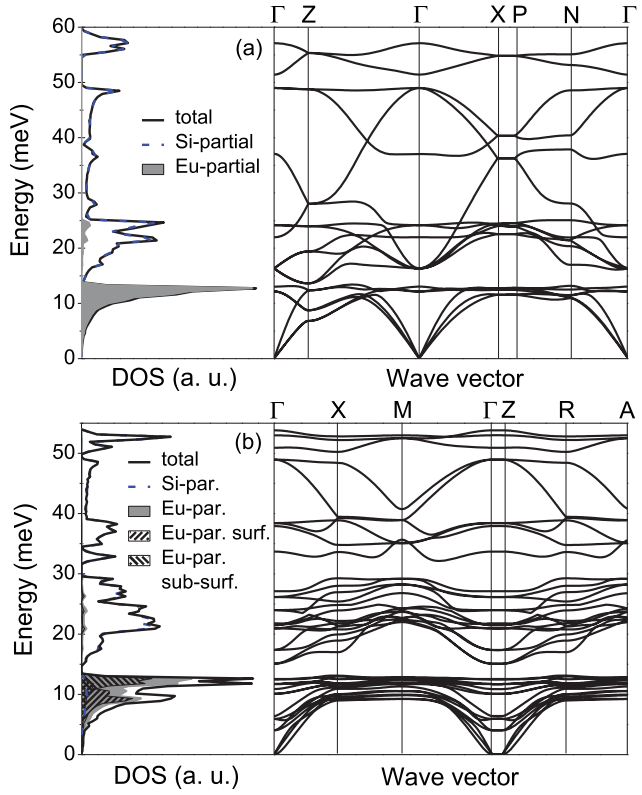

FIG. 2. The *ab initio* calculated DOS and phonon dispersions of (a) bulk $EuSi_2$ and (b) Eu-terminated $EuSi_2(001)$ slab. The high symmetry points in units of $2\pi/a$ are (a) $\Gamma = (0,0,0)$, $Z = (\frac{1}{2},0,0)$, $X = (\frac{1}{2},\frac{1}{2},0)$, $P = (\frac{1}{2},\frac{1}{2},\frac{1}{2})$, $N = (\frac{1}{2},\frac{1}{2},\frac{1}{2})$, (b) $\Gamma = (0,0,0)$, $X = (\frac{1}{3},\frac{1}{3},0)$, $M = (\frac{1}{2},0,0)$, $Z = (0,0,\frac{1}{2})$, $R = (\frac{1}{3},\frac{1}{3},\frac{1}{2})$, $A = (\frac{1}{2},0,\frac{1}{2})$. The gray area stands for the Eu-partial DOS measured in the experiment.

and bulk $EuSi_2$. Both the bulk and surface spectral features, however, exhibit a broadening that goes beyond the instrumental resolution and has another origin. In epitaxial systems with large lattice mismatch such phonon lifetime broadening could arise from strain-induced distribution of interatomic distances and has been observed in ultrathin epitaxial Fe films [10]. It can be described by the energy response of the damped harmonic oscillator function [3] with a quality factor Q, which is inversely proportional to the width of the strain field distribution [10]. Assuming a quality factor $Q = 10$ and a surface-to-volume ratio 1:3 the DOS of sample B is satisfactorily reproduced by the theory (Fig. 1). This value is about a factor of 2 smaller compared to $Q = 18$ derived for sample A, indicating the presence of residual epitaxial strain in the thin film.

The DOS of samples C and D reveal anomalous excess of states at low and high energies in addition to the bulk and surface phonon peaks (which exhibit an altered ratio due to the increased surface-to-volume ratio in the nanoislands). To understand these drastic modifications one has to consider the fact that tetragonal rare-earth disilicides are formed on the Si(001) by 45° rotation of their unit cell with respect to that of Si. In the case of $EuSi_2$ this reduces the lattice mismatch from 20.8% (expansion) to 12% (compression) [33]. The influence of the epitaxial strain field on the crystal structure and surface morphology was investigated in detail for $ErSi_2$ nanoislands and nanowires by high resolution transmission electron microscopy [44]. The analysis demonstrates that the compressive strain field accumulated at the nanoisland/Si interface (hereinafter referred to as interface 1) is gradually released at this interface and along the height of the island by developing stacking faults, misfit dislocations, distortions, and tilting of the lattice planes. These lattice defects lead to a local reduction of the force constants, consequently, to enhancement of the phonon states at low energies and broadening of the peaks [45]. Additionally, the compressive strain field relaxation at and near interface 1 results in the high-energy tail that is not present in the DOS of $EuSi_2$ with relaxed lattice. The average sizes of the islands determined by the AFM study are $50(5) \times 42(5) \times 11(2)$ and $40(5) \times 42(5) \times 9(2)$ nm^3 in sample C and D, respectively. These rather large lateral dimensions and small heights of the islands imply that a substantial fraction of atoms is located at and near the interface 1, leading to the observed anomalies in the DOS of samples C and D. The peak at 14 meV, however, has a different origin.

Another source of vibrational anomalies lies in the fact that the nanoislands in samples C and D are not isolated. Their high surface density implies the formation of interfaces between the neighboring islands (hereinafter referred to as interface 2), as depicted in Fig. 3(a). A measurable impact of this interface on the lattice dynamics is expected due to the high surface density of the nanoislands, verified by the AFM images shown in Fig. 1.

In order to evaluate the influence of these two intrinsically different interfaces on the lattice dynamics sample E, containing the same amount of Eu as sample D, was investigated. Unlike sample D, however, the growth protocol [33] of this sample ensures the formation of isolated $EuSi_2$ nanoislands with average sizes $92(5) \times 77(5) \times 22(2)$ nm^3 and very low surface density, as evidenced by the AFM image shown in Fig. 3(c). The Eu-partial DOS of samples D and E are compared in Fig. 3(d). This figure demonstrates that while at low energies the spectra are very similar for both samples, the high-energy features are distinctly different. Namely, the peak at 14 meV is suppressed and the high-energy tail is somewhat broader in the DOS of sample E. The sketch of the nanoislands arrangement in sample D, depicted in Fig. 3(a), and the AFM images shown in Figs. 3(b) and 3(c) reveal that interface 2 is the component that is not present in sample E. Hence, the differences between the phonon DOS compared in Fig. 3(d) arise essentially from the atoms located at this interface. Moreover, the grazing-incidence scattering geometry of the nuclear inelastic scattering experiment [Fig. 3(a)] ensures that the obtained

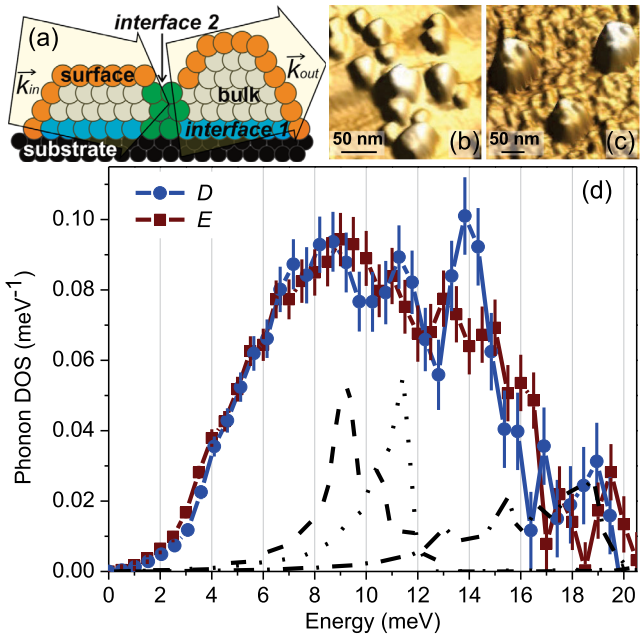

FIG. 3. (a) A sketch illustrating the islands arrangement in sample D and the grazing-incidence scattering geometry of the nuclear inelastic scattering experiment. Depicted are atoms belonging to the substrate, bulk, and surface of the islands, as well as to the interface 1 and interface 2 (see text). AFM images of samples D (b) and E (c). (d) Eu-partial DOS of samples D and E along with the *ab initio* calculated DOS of the relaxed surface (dashed line), 1.5% expanded (dotted line), and 10% compressed (dashed-dotted line) bulk $EuSi_2$ (see text).

DOS is in-plane projected, meaning that only phonons with polarization vectors parallel to the wave vector $\vec{k}_{in}$ of the incident photons contribute to the measured signal [46]. This experimental constraint implies that in addition to the vibrations of atoms located in the island interior and at their surface, atomic vibrations *along* the interface 1 are substantially contributing to the DOS of samples D and E. Furthermore, the DOS of sample D contains phonon modes arising from vibrational excitations *across* the interface 2 that are not present in the DOS of sample E. Figures 3(a) and 3(d) reveal that the localized peak at 14 meV in the DOS of sample D originates from vibrations of atoms confined within the interface 2 and having their polarization vectors normal to this interface (parallel to $\vec{k}_{in}$). Such localized high-energy modes have been predicted to arise from vibrations of spatially confined atoms within the grain boundaries of nanocrystalline materials [5,6]. Despite the observed high-energy tail in the DOS of nanoscale materials [3,7,16–18], often assigned to oxide phases [13], clear experimental evidence of this phenomenon has not yet been reported [47]. High-energy peaks arising from phonons polarized perpendicularly to the ferecrystal plane of $[(SnSe)_{1.04}]_m[MoSe_2]_n$ have recently been observed; however, they could not be unambiguously assigned to interface vibrational modes [48].

TABLE I. Experimental (expt.) and theoretical (theor.) values of the vibrational entropy S_V (k_B/atom), mean force constant F (N/m), and mean square displacement $\langle x^2\rangle$(Å^2) of the Eu atoms in $EuSi_2$ at 100 K.

		A/Bulk	Surface	B	C	D	E
S_V	Expt.	2.48(2)	⋯	2.68(2)	2.77(2)	2.83(3)	2.89(3)
	Theor.	2.43	3.02	2.61	⋯	⋯	⋯
F	Expt.	29(2)	⋯	26(2)	27(2)	28(3)	27(3)
	Theor.	29.3	19.0	26.1	⋯	⋯	⋯
$\langle x^2\rangle$	Expt.	0.009(1)	⋯	0.011(1)	0.013(2)	0.014(3)	0.015(3)
	Theor.	0.008	0.012	0.009	⋯	⋯	⋯

The broad distribution of states at high energies in the DOS of samples D and E originates from the epitaxial compressive strain field relaxation at the interface 1 and along the island height. An illustration of this effect is given by the dashed-dotted line in Fig. 3(d), which stands for the *ab initio* calculated DOS of $EuSi_2$, assuming 10% lattice compression [30]. As seen from the figure, it accounts remarkably well for the spectral features between 17 and 20 meV. Furthermore, the presence of atomic steps on the vicinal Si(001) surface induces a measurable vibrational anisotropy in the DOS of sample D and leads to the low-energy shift by about 1 meV of the bulk $EuSi_2$ peak [30].

The impact of the modified lattice dynamics of $EuSi_2$ upon transition from bulk crystal through thin film to nanoislands on selected thermoelastic properties is presented in Table I. The vibrational entropy (S_V) increases by 8% in sample B and by 14% and 17%, respectively, in samples D and E, which is among the largest deviations from bulk values of this quantity [18]. The mean force constant (F) decreases by 10% and 7%, respectively, in samples B and E. The largest deviations, however, are detected in the mean square atomic displacement ($\langle x^2\rangle$) of the Eu atoms which increases by 22% in sample B and by 56% and 67% in samples D and E, respectively, compared to the bulk value. The *ab initio* calculated Eu-partial values of the corresponding thermoelastic properties of samples A and B are in very good agreement with the experimental values. Furthermore, Table I demonstrates that the atomic vibrations of the Eu-terminated $EuSi_2(001)$ surface induce considerable deviations from the bulk values. Namely, at the surface S_V and $\langle x^2\rangle$ increase by 24% and 50%, respectively, while F decreases by 34%.

In summary, we have systematically investigated the lattice dynamics modifications in $EuSi_2$ upon transition from bulklike film through thin film to self-organized nanoislands by *in situ* nuclear inelastic scattering on ^{151}Eu and *ab initio* theory. While the Eu-partial DOS of $EuSi_2$ films can satisfactorily be described by the theory, DOS of the nanoislands exhibits anomalous enhancement of states both at low and high energies. We unambiguously demonstrate that these anomalies originate from atomic vibrations *along* the island-substrate interface owning to

the gradual release of the compressive epitaxial strain field at this interface and along the island height. Spatially confined atomic vibrations *across* the island-island interface result in high-energy modes only.

The reported results constitute an important step towards fundamental understanding of the lattice dynamics of nanoscale materials. They demonstrate that by controlling sample preparation conditions it is possible to influence atomic vibrations at the interface, thus manipulating transport and thermoelectric properties. This will have implications on the development of efficient devices for thermal management by phonon nanoengineering.

We thank B. Krause, A. Weißhardt, and H. H. Gräfe for the support in the UHV-Analysis Lab. We acknowledge ESRF-The European Synchrotron for provision of synchrotron radiation facilities, the National Isotope Development Center at Oak Ridge National Lab, which is sponsored by the U.S. DOE Basic Energy Sciences, for providing the ^{151}Eu, and the Excellence Initiative for the financial support of the UHV-Analysis Lab by the project KIT-Nanolab@ANKA. P. P. acknowledges support by the Polish National Science Center (NCN) by Projects No. 2011/01/M/ST3/00738 and No. 2012/04/A/ST3/00331. S. S. acknowledges the support by the Initiative and Networking funds of the President of the Helmholtz Association and the Karlsruhe Institute of Technology (KIT) by the Project No. VH-NG-625.

*Corresponding author.
Svetoslav.Stankov@kit.edu
†Present address: Max Planck Institute for Solid State Research, D-70569 Stuttgart, Germany.
‡On leave from Institute for Particle and Nuclear Physics, Wigner Research Centre for Physics, Hungarian Academy of Sciences, H-1525 Budapest, Hungary.
§Present address: Polytechnique Montréal, Montréal, Québec H3C 3A7, Canada.

[1] M. Stroscio and M. Dutta, *Phonons in Nanostructures* (Cambridge University Press, Cambridge, England, 2001).
[2] B. Fultz, Prog. Mater. Sci. **55**, 247 (2010).
[3] B. Fultz, C. C. Ahn, E. E. Alp, W. Sturhahn, and T. S. Toellner, Phys. Rev. Lett. **79**, 937 (1997).
[4] P. M. Derlet, R. Meyer, L. J. Lewis, U. Stuhr, and H. Van Swygenhoven, Phys. Rev. Lett. **87**, 205501 (2001).
[5] P. M. Derlet and H. Van Swygenhoven, Phys. Rev. Lett. **92**, 035505 (2004).
[6] P. M. Derlet, S. Van Petegem, and H. Van Swygenhoven, Philos. Mag. **89**, 3511 (2009).
[7] S. Stankov, Y. Z. Yue, M. Miglierini, B. Sepiol, I. Sergueev, A. I. Chumakov, L. Hu, P. Svec, and R. Rüffer, Phys. Rev. Lett. **100**, 235503 (2008); Phys. Rev. B **82**, 144301 (2010).
[8] R. Röhlsberger, W. Sturhahn, T. S. Toellner, K. W. Quast, P. Hession, M. Hu, J. Sutter, and E. E. Alp, J. Appl. Phys. **86**, 584 (1999).
[9] T. Ruckert, W. Keune, W. Sturhahn, M. Y. Hu, J. P. Sutter, T. S. Toellner, and E. E. Alp, Hyperfine Interact. **126**, 363 (2000).
[10] S. Stankov *et al.*, Phys. Rev. Lett. **99**, 185501 (2007).
[11] T. Ślęzak *et al.*, Phys. Rev. Lett. **99**, 066103 (2007).
[12] A. Kara and T. S. Rahman, Phys. Rev. Lett. **81**, 1453 (1998).
[13] L. Pasquini, A. Barla, A. I. Chumakov, O. Leupold, R. Rüffer, A. Deriu, and E. Bonetti, Phys. Rev. B **66**, 073410 (2002).
[14] A. Kara and T. S. Rahman, Surf. Sci. Rep. **56**, 159 (2005).
[15] R. Meyer, L. J. Lewis, S. Prakash, and P. Entel, Phys. Rev. B **68**, 104303 (2003).
[16] B. R Cuenya, A. Naitabdi, J. Croy, W. Sturhahn, J. Y. Zhao, E. E. Alp, R. Meyer, D. Sudfeld, E. Schuster, and W. Keune, Phys. Rev. B **76**, 195422 (2007).
[17] B. R. Cuenya, J. R. Croy, L. K. Ono, A. Naitabdi, H. Heinrich, W. Keune, J. Zhao, W. Sturhahn, E. E. Alp, and M. Hu, Phys. Rev. B **80**, 125412 (2009).
[18] B. R. Cuenya *et al.*, Phys. Rev. B **86**, 165406 (2012).
[19] U. Stuhr, H. Wipf, K. H. Andersen, and H. Hahn, Phys. Rev. Lett. **81**, 1449 (1998).
[20] N. Spiridis *et al.*, Phys. Rev. Lett. **115**, 186102 (2015).
[21] B. R. Cuenya *et al.*, Phys. Rev. B **77**, 165410 (2008).
[22] C. Colvard, R. Merlin, M. V. Klein, and A. C. Gossard, Phys. Rev. Lett. **45**, 298 (1980).
[23] A. K. Sood, J. Menéndez, M. Cardona, and K. Ploog, Phys. Rev. Lett. **54**, 2111 (1985); **54**, 2115 (1985).
[24] M. Maldovan, Nature (London) **503**, 209 (2013).
[25] M. Maldovan, Nat. Mater. **14**, 667 (2015).
[26] C. Preinesberger, S. Vandré, T. Kalka, and M. Dähne-Prietsch, J. Phys. D **31**, L43 (1998).
[27] D. E. Chang, A. S. Sørensen, P. R. Hemmer, and M. D. Lukin, Phys. Rev. Lett. **97**, 053002 (2006).
[28] G. M. Snider and R. S. Williams, Nanotechnology **18**, 035204 (2007).
[29] D. V. Averyanov, A. M. Tokmachev, C. G. Karateeva, I. A. Karateev, E. F. Lobanovich, G. V. Prutskov, O. E. Parfenov, A. N. Taldenkov, A. L. Vasiliev, and V. G. Storchak, Sci. Rep. **6**, 25980 (2016).
[30] See Supplemental Material at http://link.aps.org/supplemental/10.1103/PhysRevLett.117.276101 for samples preparation and characterization, vibrational anisotropy, and *ab initio* calculations, which includes Refs. [31,32].
[31] J. P. Perdew, K. Burke, and M. Ernzerhof, Phys. Rev. Lett. **77**, 3865 (1996).
[32] P. E. Blöchl, Phys. Rev. B **50**, 17953 (1994).
[33] A. Seiler, O. Bauder, S. Ibrahimkutty, R. Pradip, T. Prüßmann, T. Vitova, M. Fiederle, T. Baumbach, and S. Stankov, J. Cryst. Growth **407**, 74 (2014).
[34] S. Ibrahimkutty, A. Seiler, T. Prüßmann, T. Vitova, R. Pradip, O. Bauder, P. Wochner, A. Plech, T. Baumbach, and S. Stankov, J. Synchrotron Radiat. **22**, 91 (2015).
[35] M. Seto, Y. Yoda, S. Kikuta, X. W. Zhang, and M. Ando, Phys. Rev. Lett. **74**, 3828 (1995).
[36] W. Sturhahn, T. S. Toellner, E. E. Alp, X. Zhang, M. Ando, Y. Yoda, S. Kikuta, M. Seto, C. W. Kimball, and B. Dabrowski, Phys. Rev. Lett. **74**, 3832 (1995).
[37] S. Stankov, R. Rüffer, M. Sladecek, M. Rennhofer, B. Sepiol, G. Vogl, N. Spiridis, T. Slezak, and J. Korecki, Rev. Sci. Instrum. **79**, 045108 (2008).
[38] R. Rüffer and A. I. Chumakov, Hyperfine Interact. **97**, 589 (1996).

[39] O. Leupold, J. Pollmann, E. Gerdau, H. D. Rüter, G. Faigel, M. Tegze, G. Bortel, R. Rüffer, A. I. Chumakov, and A. Q. R Baron, Europhys. Lett. **35**, 671 (1996).

[40] R. P. Hermann, R. Jin, W. Schweika, F. Grandjean, D. Mandrus, B. C. Sales, and G. J. Long, Phys. Rev. Lett. **90**, 135505 (2003).

[41] J. Evers, G. Oehlinger, and A. Weiss, J. Solid State Chem. **20**, 173 (1977).

[42] G. Kresse and J. Furthmüller, Comput. Mater. Sci. **6**, 15 (1996).

[43] K. Parlinski, Z. Q. Li, and Y. Kawazoe, Phys. Rev. Lett. **78**, 4063 (1997).

[44] T. Ding, Y. Wu, J. Song, J. Li, H. Huang, J. Zou, and Q. Cai, Nanotechnology **22**, 245707 (2011).

[45] Similar phonon softening and peaks broadening due to local crystal defects were observed in strongly distorted FeO; see U. D. Wdowik, P. Piekarz, K. Parlinski, A. M. Oleś, and J. Korecki, Phys. Rev. B **87**, 121106 (2013).

[46] A. I. Chumakov and W. Sturhahn, Hyperfine Interact. **123/124**, 781 (1999).

[47] Observation of individual peaks is limited by the energy resolution and statistical significance of the data.

[48] B. Klobes, M. Y. Hu, M. Beekman, D. C. Johnson, and R. P. Hermann, Nanoscale **8**, 856 (2016).